Sulfonated Ion Exchange Polystyrene Composite Resin for Calcium Hardness Removal

Mahmoud Fathy[1], Th. Abdel Moghny[2], Mahmoud Ahmed Mousa[3], Abdel-Hameed A-A. El-Bellihi[4], Ahmed E. Awadallah[5]

[1, 2]*Applications Department, Egyptian Petroleum Research Institute (EPRI), 1 Ahmed El-Zomer, Nasr City, Box. No. 11727, Cairo, Egypt*
[3,4]*Faculty of Science Benha University, Fred Nada Street, - Banha – Cairo, Egypt*
[5]*Development of processes Department, Egyptian Petroleum Research Institute, 1 Ahmed El-Zomer, Nasr City, Box. No. 11727, Cairo, Egypt*

Abstract-- The nanocomposite cation exchange resins were synthesized throwing a waste polystyrene sulfonate (WPSS) arrange with nano estimated structures of an amorphous carbon film. The synthesis and acidified amorphous carbon film with waste polystyrene nanoparticles were carried out using solvent evaporation in micro emulsion technique as a new strategy. In this respect, self-assembled amorphous carbon film /waste polystyrene (ACTF/WPS) hybrid nanocomposite were prepared by solvent evaporation using micro emulsion polymerization. The ACTF was used as filler in a host polystyrene matrix to form composite resins. The chemical and crystalline structure of polymers and nanocomposite has been proven by studies the FTIR spectrum, X- rays and thermal analysis. SEM and TEM analysis to study morphology of resin and amorphous carbon that assembled with polystyrene chain. The synthetic similarity of the pitch and the amorphous carbon film give stable nanocomposite with up to 1 wt.% ACTF. The WPSS/ amorphous carbon film composite pitch has more prominent particle trade limit than WPSS resin. The composite resins are thermally stable and show case higher chemical stability in an ion exchange process than the WPSS resins. The lessened rate of debasement of the nanocomposite resin recommends that with further development they may have anew potential applications as water treatment process.

Keywords- composites; Polymer; resin; solvent evaporation; amorphous carbon

I. INTRODUCTION

An ion-exchange resin or ion-exchange polymer is an insoluble matrix normally as small beads, usually white or yellowish, fabricated from an organic polymer substrate. Ion-exchange resins are widely used in different separation, purification, and decontamination processes[1]. Cross linking decreases ion-exchange capacity of the resin and prolongs the time needed to accomplish the ion exchange processes but improves the robustness of the resin[2]. Specialized ion exchange resins are also known such as chelating resins. Anion and cation resins are the two most common resins used in the ion exchange process.

Cations are replaced with hydrogen ions (positively charged ions) using cation-exchange resins; anions are replaced with hydroxyls (attract negatively charged) using anion-exchange resins. The resin contact with solution containing magnesium and calcium ions, the magnesium and calcium ions preferentially migrate out of solution to the active sites on the resin, being replaced in solution by sodium ions[3, 4]. The resin can be recharged by washing it with a solution containing a high concentration of sodium ions dissolved in it. One application of ion-exchange resins that using it to remove poisonous and heavy metal ions from polluted water, with exchanging them with more other safe ions, such as sodium, hydrogen and potassium ions. There are some ions-exchange resins that do remove organic ions, such as acrylate resins[5]. Hard drinking water is generally not harmful to human health, but can pose serious problems in industrial settings, where water hardness is monitored to avoid costly breakdowns in boilers, cooling towers, and other equipment that handles water[6]. Thus be defined as the soap-consuming capacity of a water sample, or the capacity of precipitation of soap as a characteristic property of water that prevents the lathering of soap. Hard water also forms deposits that clog plumbing. These deposits, called scale, are composed mainly of calcium carbonate, magnesium hydroxide [7, 8], and calcium sulfate. Calcium and magnesium carbonates are deposited as off-white solids on the inside surfaces of pipes and heat exchangers. The presence of ions in an electrolyte, in this case, hard water, can also lead to galvanic corrosion, in which one metal will preferentially corrode when in contact with another type of metal, when both are in contact with an electrolyte. In swimming pools, hard water is manifested by a turbid, or cloudy, appearance to the water [9-11]. Where softening is practiced, it is often recommended to soften only the water sent to domestic hot water to prevent or delay inefficiencies and damage scale formation in water heaters[12].

A common method for water softening involves the use of ion exchange resins, which replace ions like Ca^{2+} by twice the number of mono cations such as sodium or potassium ions.

In this paper, we prepared composite cation exchange resin contain ACTF as nano carbon structures. Waste Polystyrene sulfonate (WPSS) resin will prepare from styrene polymer (polystyrene) with the amorphous carbon thin film. The amorphous carbon thin film makes the polymer more flexible, which is necessary to give a good contact with the electrolytes.

II. EXPERIMENTAL

2.1. Materials

The inorganic chemicals including $CaCl_2 \cdot 2H_2O$, HCl, and NaOH were obtained from Merck (Darmstadt, Germany) in analytical grade. All solutions were prepared using distilled water.

2.2. Pretreatments of rice straw

Rice straw was subjected to pretreatment process. Hence, hemicellulose was solubilized as monomeric sugars during the dilute acidic hydrolysate process using 1% (wt/wt) sulphuric acid at 120^oC for 60 minutes. The resulting residue subjected to succeeding delignification process to remove lignin at 120^0C for 60 minutes using a mixture of 1.5% (wt/wt) NaOH and 0.5% (wt/wt) H_2O_2.

2.3. Preparation of Cobalt Silicate Nanoparticles

A cobalt silicate nanoparticle was prepared according to Stöber et al. method [11]. In this respect, 4.0g of the freshly prepared cobalt nitrate and silica was vigorously stirred with 200ml of ethanol for 30 minutes at 45°C, after that 40ml water, and 4ml (1.4M) NaOH was added to the above suspension. Then the powder was separated and being to dry at 50°C for 8h in a vacuum oven.

2.4. Preparation Amorphous Carbon Thin Film (ACTF)

5 grams of cellulose obtained from treated rice straw were added to 5ml concentrated sulfuric acid in the presence of 0. 1g silica and stirred for 10 minutes, then filtrated and washed by hot water until pH 7 and saving in oven at 40^oC for 6 hours. The prepared semi carbonized cellulose was poured into the flask in presence of 0.01g cobalt silicate nanoparticle and heated up to 40^oC for 30 minutes. The prepared amorphous carbon thin film (ACTF) left to cool for one hour, then dried in a vacuum oven for 24 hours at $50-70^oC$.

2.5. Preparation of self-assembled amorphous carbon film /waste polystyrene hybrid nanocomposite

10 g of waste polystyrenes was solubilized in 5ml toluene, and then added 1% from total carbon nanotubes and mixing for 30 minutes using the ultrasonic apparatus for 20 minutes at 30°C and 1000 Watt electric capacity. After that, black carbon nanotube suspensions folded by long and short polystyrene chain were obtained by strong non covalent bond. Later, 0.5 wt/wt of sodium dodecyl sulphate was completely dissolved in 500ml distilled water, and mix properly with 0.1 wt/wt hydroxyl propyl cellulose for 20 minutes, after that slowly add organic solution to an aqueous solution with stirring at 900 rpm speed for four hours and at 80°C, a solid polystyrene with carbon deposit resins was obtained. Such solid was subjected to wash well with hot water and then dried for 24 hours at 40°C.

2.6. Sulfonation of Ion-Exchange Resin

20.4 g of waste polystyrene was put in a bottom glass flask reactor (500 cm 3) equipped with mechanical agitation, vertical condenser, and thermometer. The flask containing the solution was heated in the silicone oil bath to 48— 52 °C. Acetyl sulfate as sulfonating agent was prepared in a separate flask: 12.0 cm ^{3} of acetic anhydride was added carefully to 6.0 cm ^{3} of 95—97% sulfuric acid. The prepared acetyl sulfate was poured through the vertical condenser to the solution of WPSS resins. The reaction mixture was heated to about 35 °C and stirred for 1 h. Then the sulfonated WPS resins was isolated and dried in oven for 24 h at 30^0C.

2.7. Preparing of the Solutions of Synthetic Hard Water

1000ml of synthetic hard water solution have been prepared as stock solution. afterwards 950mL of such as solution was adjusted at certain pH value and then transferred to the 1L volumetric flask and completed by distilled water to the mark [14, 15].

2.8. Effect of Contact Time

5. 0g of the resin was mixed with 100ml of synthetic hard water solution with stirring rate at 200rpm in the pH range between 2.0 and 5.0. The equilibrium of contact time was established for 60 minutes [14, 16].

2.9. Effect of pH

The sorption of Ca (II) ions and removal of hardness from hard water solution were studied with the waste polystyrene cation exchange resins [H$^+$] at initial pH ranges between 2.0 and 5.0.

The initial pH of the solution of hard water was controlled with pH meter by adding solutions of hydrochloric acid and sodium hydroxide. In the experiment, the temperature, stirring speed, and maximum contact time were kept constant at 298K and 200rpm for 60 minutes [17-19].

2.10. Effect of resin weight

The adsorption of calcium ions from aqueous media was studied at varying amount of waste polystyrene resin lay between 0.025 to 0.350 g at pH 7.0±0.1, taken in consideration that the best resin dosage was fixed as 0.3g [14].

III. RESULT AND DISCUSSION

3.1. FTIR analysis

From the FTIR spectra of non crystalline, amorphous carbon Figure (1), we found a band at 3659 cm^{-1} indicating to the presence of the OH functional group, and a band at 1100 cm^{-1} indicating the presence of the C=O stretching beyond. Generally, carbon shape in every stereochemistry has formed always poor marks in the infrared unless it's chemically treated with oxidation [20].
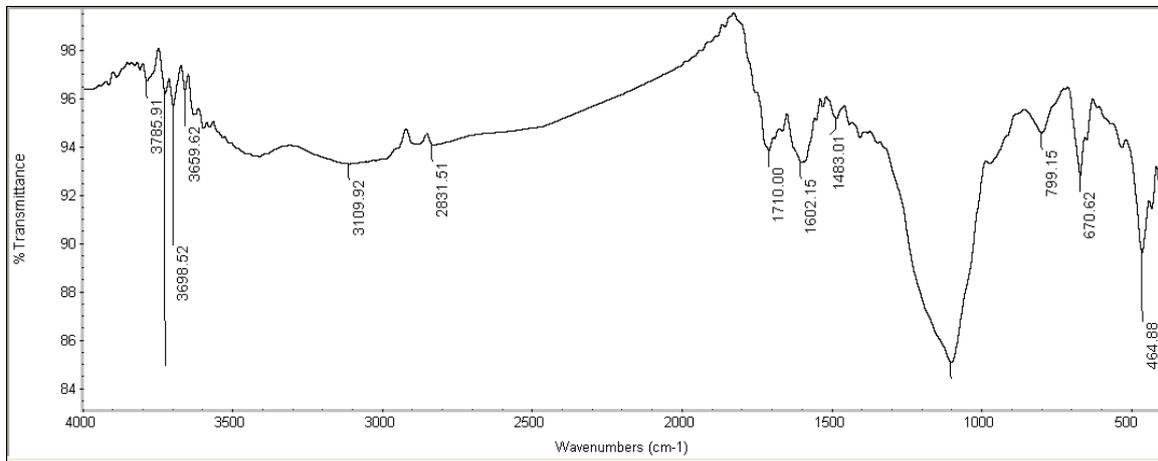

Figure.1. FTIR analysis of amorphous carbon film

The FTIR spectra of polystyrene/amorphous carbon resin in Figure (2) exhibited the characteristic bands at 697, 1449 and 1491 cm^{-1} represents the mono substituted aromatic ring of polystyrene/amorphous carbon. The bending vibration band of the polystyrene ring in the plane and appears at 1027 cm^{-1} [21].

Also Figure 2 shown the fairly broad band at about 3460 cm^{-1} that assigned to the bending vibration of the OH group, which was probably caused by the drifting of its stretching, vibration toward the low-frequency direction, under the hydrogen bond interaction between the H_2O molecule and the oxygen atom of the amorphous carbon [22].
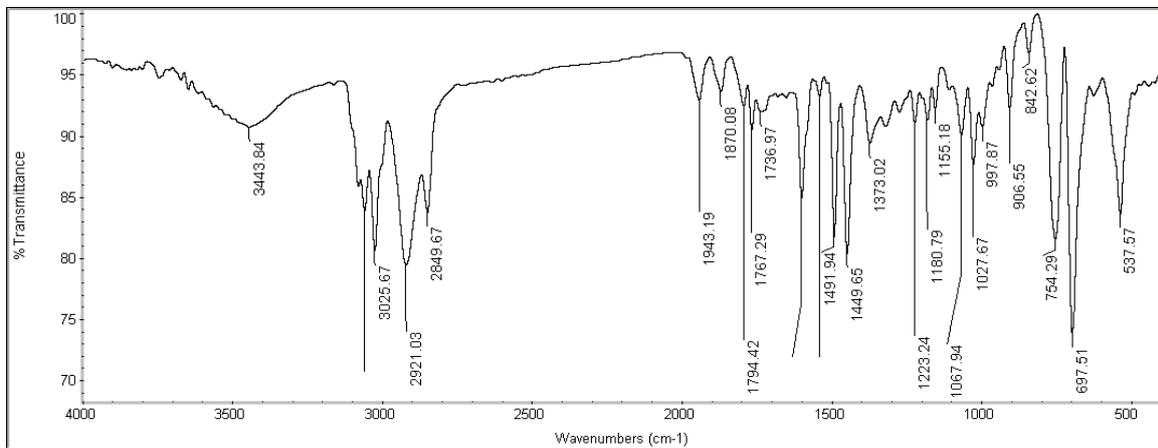

Figure.2. FTIR analysis of amorphous carbon film/waste polystyrene resin

3.2. X-ray analysis

The X-rays pattern in Figure 3 shows the high crystallinity of transparent amorphous carbon thin films with characteristic peaks at 20 $^\circ$, 25 $^\circ$ at 2θ that corresponding to the graphitic structure of transparent amorphous carbon thin films [23].
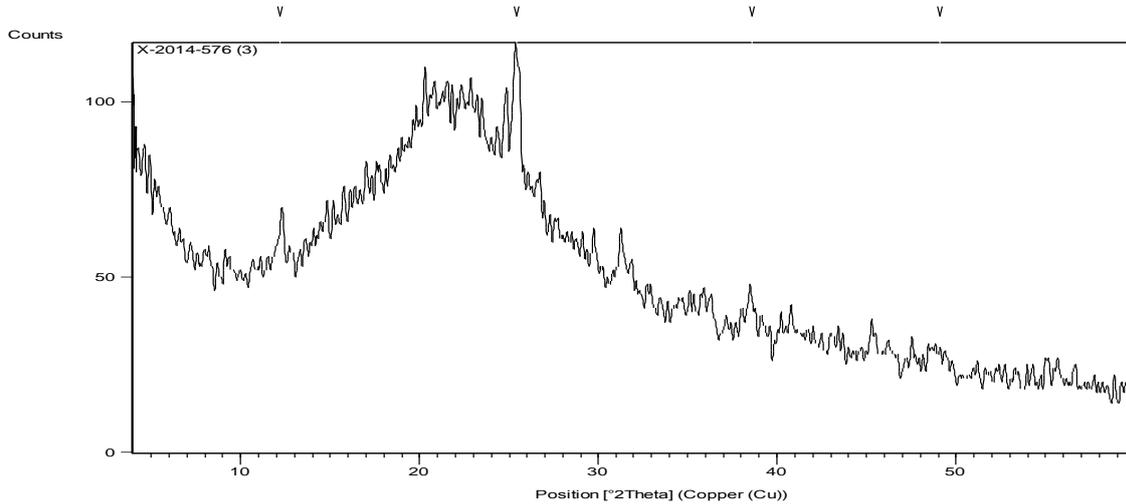

Figure.3.X-ray analysis of amorphous carbon film

In Figure 4, the amorphous peak at 20° indicated the presence of silica nanoparticles at sizes reach to 50nm and the presence of transparent amorphous carbon thin films peaks. I/we know that the decreased size of the prepared nanoparticles leads to appear of a broad amorphous band more than sharp crystalline one [24].

As expected, they cannot be assigned to crystalline melting, because X-ray diffraction analysis of PS/amorphous carbon film samples shows that its amorphous form. This behavior cannot be assigned to the melting of pure PS either, because PS is also amorphous.
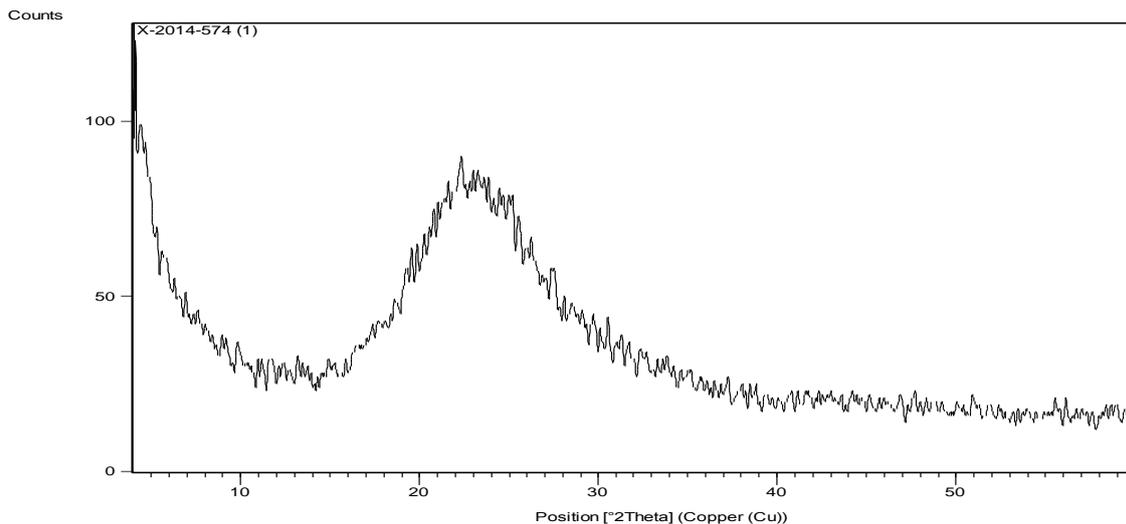

Figure.4. X-ray analysis of amorphous carbon film/waste polystyrene resin

3.3. Thermal analysis

The thermal stabilities of amorphous carbon film given in Figure 5 included three steps, the first one for the residual water and ending at 100°C, the second step started at 100°C and ending at 500°C because decarbonation of the carbon skeleton of amorphous carbon film, the last step at 550°C and ending nearly at 800°C given that evaporation of carbon dioxide gas with 30% residual as catalyst nanoparticle. The thermal stabilities of the waste base polymer polystyrene and nanocomposites were studied under air atmosphere by thermal gravimetric analysis.

The results presented in Figure (6) show that the samples have three main weight loss peaks, the first weight-loss step at low temperature is mainly due to evaporation of residual ethanol, water, toluene and/or the sulfonic groups, the second step started at 200°C and ending at 400°C [25], this means that about 99.8% of total sample decomposed and the remaining is the third step and equal to 0.11%, the results are superb agreement with as mentioned by [26]. The thermal stabilities of amorphous carbon film/waste polystyrene resin shown in Figure 7 exhibited an increase in thermal stability of composite polymer as compared with the corresponding waste polystyrene. Composite polymer shows a weight loss process with its onset at about 500°C. The degradation process is better visualized and takes place in two main steps.
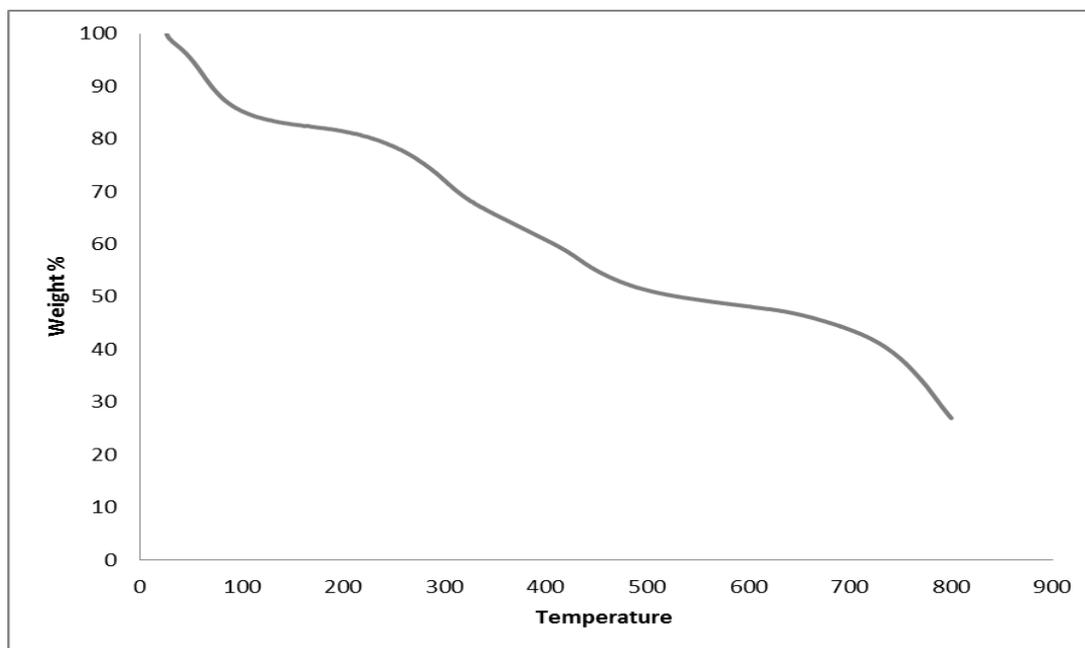

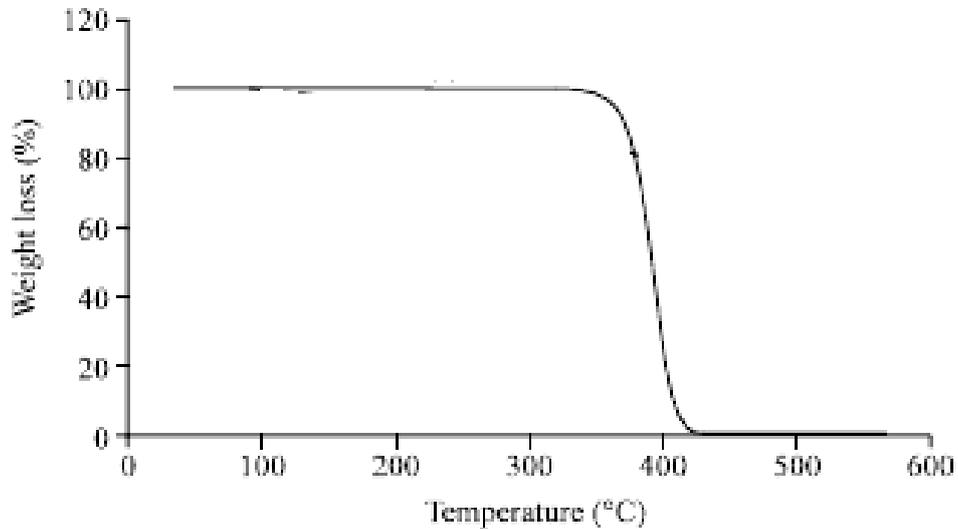**Figure.5. TGA analysis of amorphous carbon film**

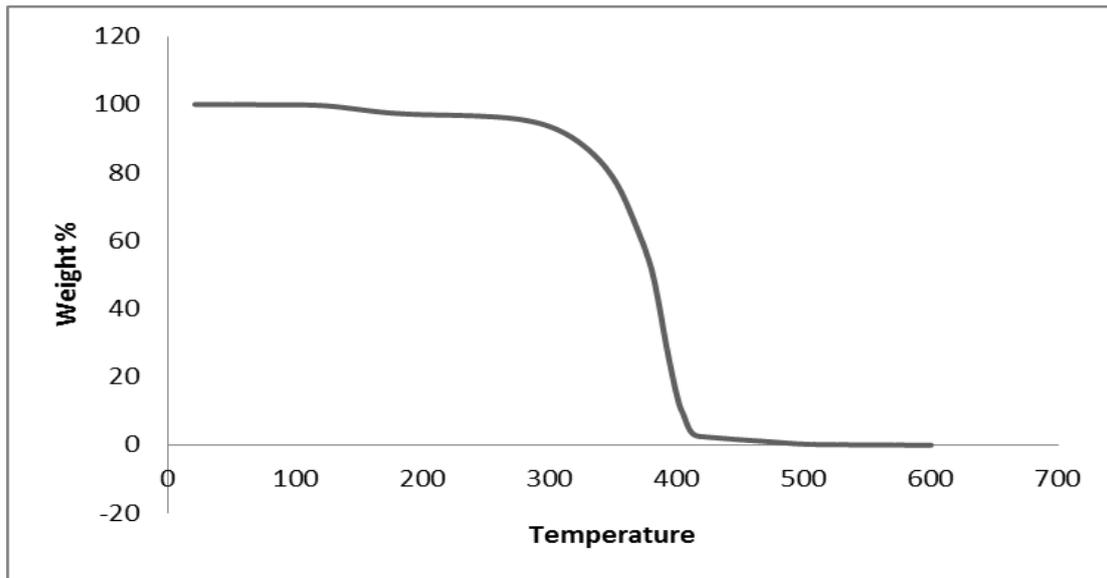**Figure.6. TGA analysis of waste polystyrene resin**

Figure.7. TGA analysis of amorphous carbon film/waste polystyrene resin

3.4. High Resolution Transmission Electron Microscope (HRTEM) and Selected Area Electron Diffraction (SAED) Analysis

HRTEM images revealed that the transparent amorphous carbon thin films comprised irregular aggregated, thin, crumpled sheets closely associated with each other and forming a disordered solid as shown in Figure 8. The folded regions of the sheets have average widths of 2 nm this indicates the presence of individual sheets in the prepared transparent amorphous carbon thin films.

Also show that the preparation of transparent amorphous carbon thin films using a new chemical treatment process without the presence of cobalt silicate nano particle gives highly graphene orders with low cross linked layer above and lower the original graphene sheet. The SAED pattern in Figure 9 shows only weak and diffuse rings, indicating that the prepared transparent amorphous carbon thin films in the form of amorphous structure. It is expected that the stacking sheets of transparent amorphous carbon thin films since Vander Waals's attractive interactions, with a random arrangement.
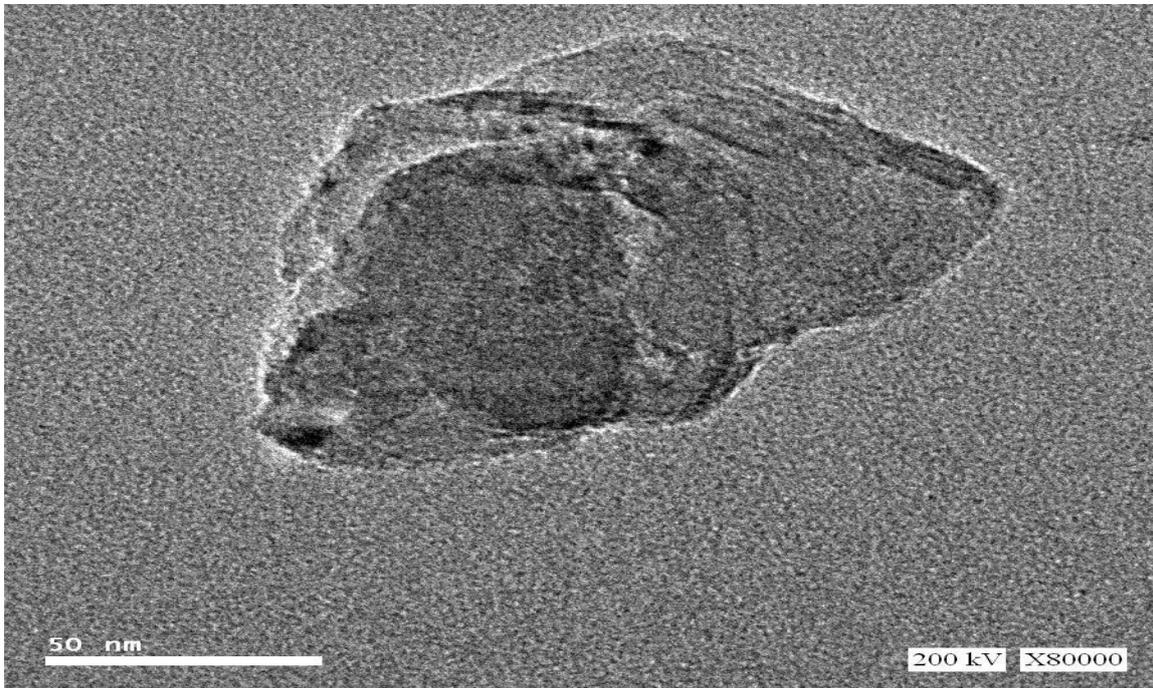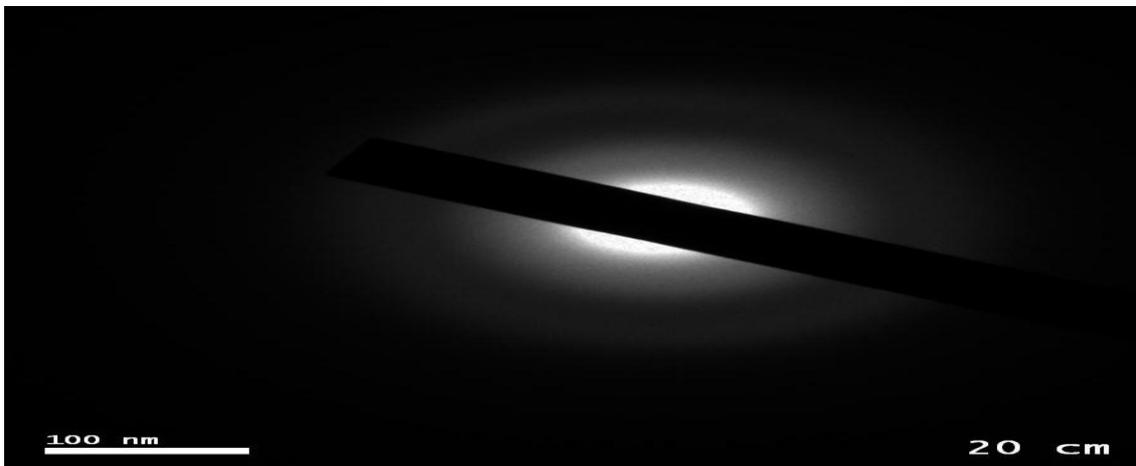
Figure 8. HRTEM analysis of amorphous carbon film

Figure 9. SAED analysis of amorphous carbon film

3.5. SEM analysis

Figure 10 shows the amorphous carbon film is penetrated inside the composite polymer that comprises polystyrene as the matrix than that in the outer surface of the resin, this because the polymer chain is folded on the amorphous carbon film.

This can be explained by non-covalently bond between polymers and amorphous carbon film, which in turn affected the thermal stability of prepared nano composite. The top left regions in Figure 9 shows the emerged of carbon film inside the resin and covered for all aspects, and this shows the compatibility between polymers and nano amorphous carbon film.
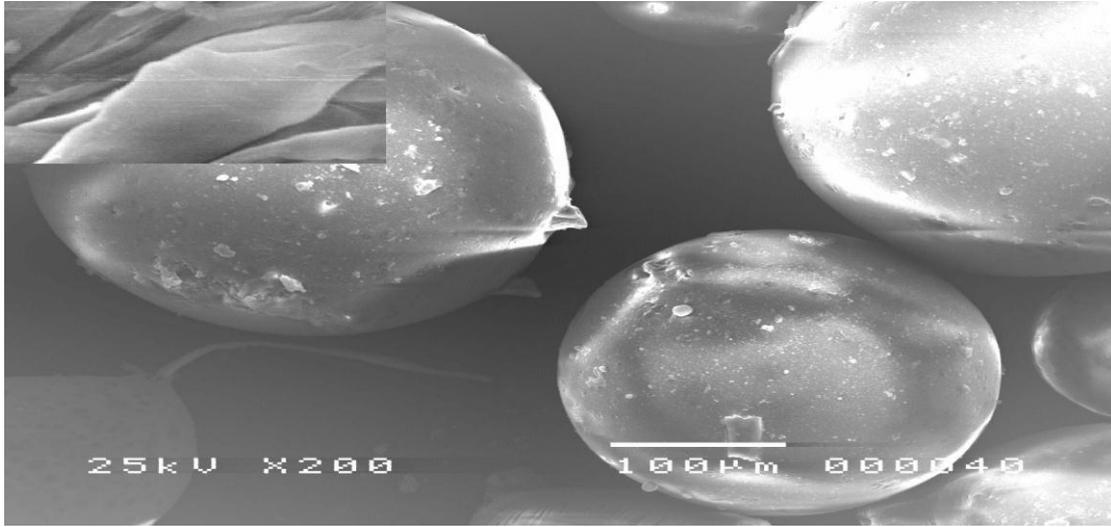
Figure.10.SEM analysis of amorphous carbon film/waste polystyrene resin

3.6. Contact time

Through the contact time study, we found that the resins prepared by the new sulfonation process have very high adsorption susceptibility toward the calcium ion when comparing with the earlier studies, whereas, the prepared resins absorb 400 mg of calcium ion in the first ion-exchange process minutes.

The stable ion-exchange dynamic state reached to the final saturation of the ion-exchange active site with the very weak dynamic exchange process [14]. The dynamic stage starts at 20 minutes hence the dynamic exchange occurs between ions into the solution and resins [2, 27].
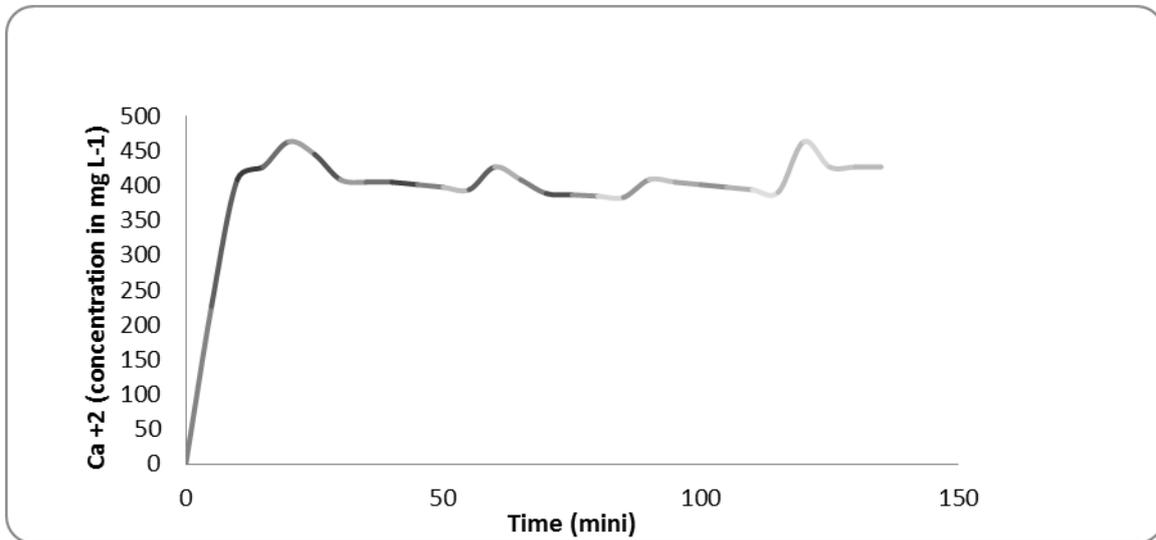

Figure 11 Effects of Contact Time between Resin and Synthetic Solution of Hard Water on Removal of Hardness of Calcium.

3.7. Effect of pH

Effect of pH on the removal of calcium ion from synthetic hard water solution is given in Figure (12), it's clear that the adsorption of calcium ion values are highest in the basic media than in acidic one because there is an abundance of hydrogen ions in solution, which is considered as competitive ion with calcium ion.

It appears from the Figure that the lowest ion-exchange process value got at 300 mg /L where in the neutral pH media the ion-exchange value lie between 300-450 mg /L and reach to the highest value in the basic media at500 mg /L [18]. Through these pH results, one can suggest that the rank of cationic exchange column can be lay before anion exchange resin that in the process of brackish water soften.
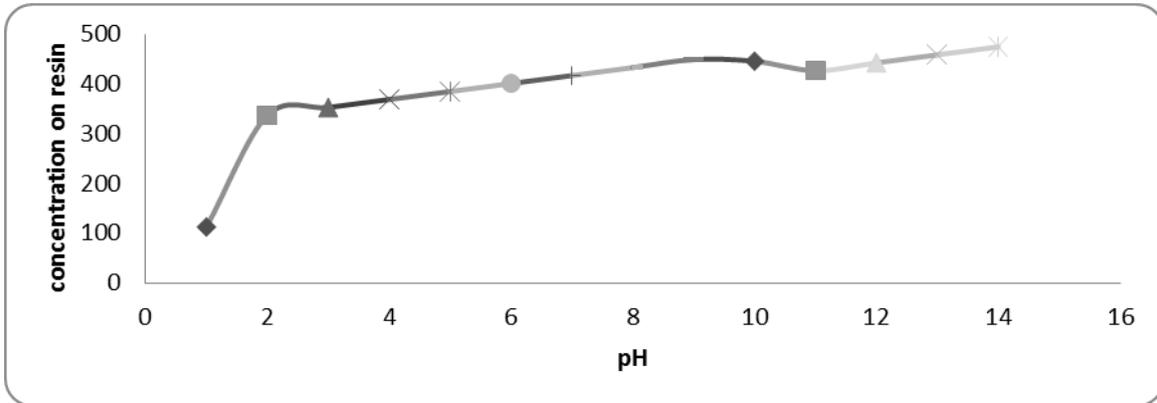
Figure 12 Effects of pH on Removal of Hardness of calcium

3.8. *Effect of resin dosage:*

It's evidenced from Figure (13) that the amount of resin necessary to remove the existing calcium ion (450 mg/l) from synthetic hard water is 0.2 grams, which is tiny in comparing with the concentration of calcium ions present in the brackish water.

We found that the prepared resins have the ability to remove the calcium ions by 98% at neutral pH at 0.2 mg of resins. It's also clear that after that weight the dynamic equilibrium reached because of active site saturation that presence on the resins surfaces [18].
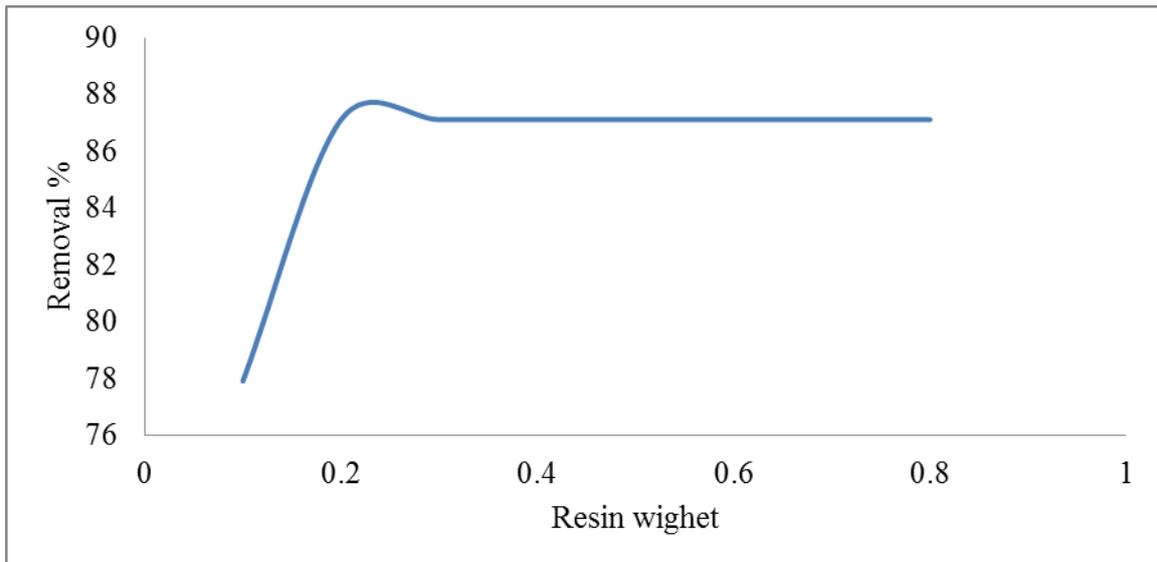

Figure 13 the effect of resin dosage on the exchange of calcium ion by sulfonated waste polystyrene resin

IV. CONCLUSION

The interaction in the nanocomposite between the amorphous carbon films and WPS provided the thermal properties, the prepared nanocomposite resin. Such a structure improves mechanical and thermal properties of waste polystyrene resin. In this study, the matrix of waste polystyrene will sulfonated by acetyl sulfate reagent, then resin use was developed to remove the calcium ions from brackish water through dynamic studies such as time, pH and the amount of the resin.

The addition of amorphous carbon film into WPS causes a reinforcement effect since both ion-exchange capacity and calcium removal have been improved in the nanocomposite. We found that the prepared resins can remove the calcium ions by 98% at neutral pH at 0.2 mg of resins. Therefore, its advised to use such resins for desalination of brackish water from calcium ion.

Overall, this new hybrid nanostructure has the potential to combine the major advantages of amorphous carbon films to produce significant improvement in their current application's as ion exchange resin that used in water softener. The cation exchange resin is nonporous to permit water and calcium ions to diffuse through the ACTF network. The presence of the amorphous carbon film in the composite resin increases the cation exchange capacity, decreases the swelling of resins with water around it, and reduces the rate of degradation by environment. It is thermosetting and insoluble in solvent and it has a low-cost.

REFERENCES

[1] Zhu, Y., et al., Adsorption of perchlorate from aqueous solutions by anion exchange resins: Effects of resin properties and solution chemistry. Colloids and Surfaces A: Physicochemical and Engineering Aspects, 2015. **468**(0): p. 114-121.

[2] Mahmoud, M.A., Kinetics and thermodynamics of aluminum oxide nanopowder as adsorbent for Fe (III) from aqueous solution. Beni-Suef University Journal of Basic and Applied Sciences, (0).

[3] Wang, J., et al., Effect of pore structure on adsorption behavior of ibuprofen by magnetic anion exchange resins. Microporous and Mesoporous Materials, 2015. **210**(0): p. 94-100.

[4] Basavarajappa, H.T. and M.C. Manjunatha, Groundwater Quality Analysis in Precambrian Rocks of Chitradurga District, Karnataka, India Using Geo-informatics Technique. Aquatic Procedia, 2015. **4**(0): p. 1354-1365.

[5] Shen, S., et al., Adsorption of Pd(II) complexes from chloride solutions obtained by leaching chlorinated spent automotive catalysts on ion exchange resin Diaion WA21J. Journal of Colloid and Interface Science, 2010. **345**(1): p. 12-18.

[6] Quinta Ferreira, R.M. and A.E. Rodrigues, Diffusion and catalytic zero-order reaction in a macroreticular ion exchange resin. Chemical Engineering Science, 1993. **48**(16): p. 2927-2950.

[7] Chicot, D., et al., Hardness of thermal sprayed coatings: Relevance of the scale of measurement. Surface and Coatings Technology, 2015. **268**(0): p. 173-179.

[8] Yang, H., et al., Magnetic prussian blue/graphene oxide nanocomposites caged in calcium alginate microbeads for elimination of cesium ions from water and soil. Chemical Engineering Journal, 2014. **246**(0): p. 10-19.

[9] Vecino, X., et al., Study of the physical properties of calcium alginate hydrogel beads containing vineyard pruning waste for dye removal. Carbohydrate Polymers, 2015. **115**(0): p. 129-138.

[10] Zhao, J., et al., Biomimetic and bioinspired membranes: Preparation and application. Progress in Polymer Science, 2014. **39**(9): p. 1668-1720.

[11] Simate, G.S. and S. Ndlovu, Acid mine drainage: Challenges and opportunities. Journal of Environmental Chemical Engineering, 2014. **2**(3): p. 1785-1803.

[12] Laxman, K., et al., Desalination and disinfection of inland brackish ground water in a capacitive deionization cell using nanoporous activated carbon cloth electrodes. Desalination, 2015. **362**(0): p. 126-132.

[13] Zhang, R., et al., Assembly of graphene and nickel nanoparticles on anion exchange resin microspheres for the amperometric detection of carbohydrates in combination with capillary electrophoresis. Journal of Chromatography A, 2014. **1374**(0): p. 261-267.

[14] Mahmoud Fathy, T.A.M., M. M. Abdou , Abdel-Hameed A-A. El-Bellihi , and Ahmed E. Awadallah, Study the Adsorption of Ca (II) and Mg (II) on High Cross-Linked Polystyrene Divinyl Benzene Resin. International Journal of Modern Chemistry, 2015. **7** (1): p. 36-44

[15] Nielsen, A.D., C.C. Fuglsang, and P. Westh, Isothermal titration calorimetric procedure to determine protein–metal ion binding parameters in the presence of excess metal ion or chelator. Analytical Biochemistry, 2003. **314**(2): p. 227-234.

[16] Ma, W., et al., Adsorption and bio-sorption of nickel ions and reuse for 2-chlorophenol catalytic ozonation oxidation degradation from water. Journal of Hazardous Materials, 2014. **266**(0): p. 19-25.

[17] Mahmood, N., et al., Preparation of bio-based rigid polyurethane foam using hydrolytically depolymerized Kraft lignin via direct replacement or oxypropylation. European Polymer Journal, 2015. **68**(0): p. 1-9.

[18] Mahmoud fathy, T.A.M., Ahmed E. Awad Allah , M. M. Abdou , and Abdel-Hameed A-A Fl-Bellihi, , Kinetic Study of Ca(II) And Mg(II) on High Crosslinked PS-DVB Synthetic Resin from Chromium Solution. International Journal of Modern Organic Chemistry, 2015. **4**(1): p. 40-45.

[19] Janković, B., M. Marinović-Cincović, and M. Dramićanin, Kinetic study of isothermal crystallization process of Gd2Ti2O7 precursor's powder prepared through the Pechini synthetic approach. Journal of Physics and Chemistry of Solids, 2015. **85**(0): p. 160-172.

[20] Zuyi, T., Z. Hui, and Z. Baolin, Thermodynamic functions for ion exchange of amino acid. Reactive and Functional Polymers, 1995. **27**(1): p. 29-33.

[21] Trautmann, M., S. Lubahn, and H.-J. Holdt, Preparation, characterisation and properties of sulphoxide modified polystyrene resins for solid-phase extraction of PtIV, RuIII and RuIV from hydrochloric acid. Reactive and Functional Polymers, 2014. **83**(0): p. 84-97.

[22] Pan, B., et al., Acid and organic resistant nano-hydrated zirconium oxide (HZO)/polystyrene hybrid adsorbent for arsenic removal from water. Chemical Engineering Journal, 2014. **248**(0): p. 290-296.

[23] Maicaneanu, A., et al., Physical-chemical and electrochemical characterization of Fe-exchanged natural zeolite applied for obtaining of hydrogen peroxide amperometric sensors. Chemie der Erde - Geochemistry, 2014. **74**(4): p. 653-660.

[24] Alonso-Fagúndez, N., et al., Poly-(styrene sulphonic acid): An acid catalyst from polystyrene waste for reactions of interest in biomass valorization. Catalysis Today, 2014. **234**(0): p. 285-294.

[25] Cantalapiedra, A., et al., Electrochemical sensor based on polystyrene sulfonate–carbon nanopowders composite for Cu (II) determination. Talanta, 2015. **139**(0): p. 111-116.

[26] Karimi, A., et al., Functional group effect on carbon nanotube (CNT)-supported cobalt catalysts in Fischer–Tropsch synthesis activity, selectivity and stability. Fuel, 2014. **117, Part B**(0): p. 1045-1051.

[27] Mahmoud, A.M., et al., Adsorption of heavy metal ion from aqueous solution by nickel oxide nano catalyst prepared by different methods. Egyptian Journal of Petroleum, 2015. **24**(1): p. 27-35.

Corresponding author: fathy8753@yahoo.com, dr.abo_fathy@yahoo.com